



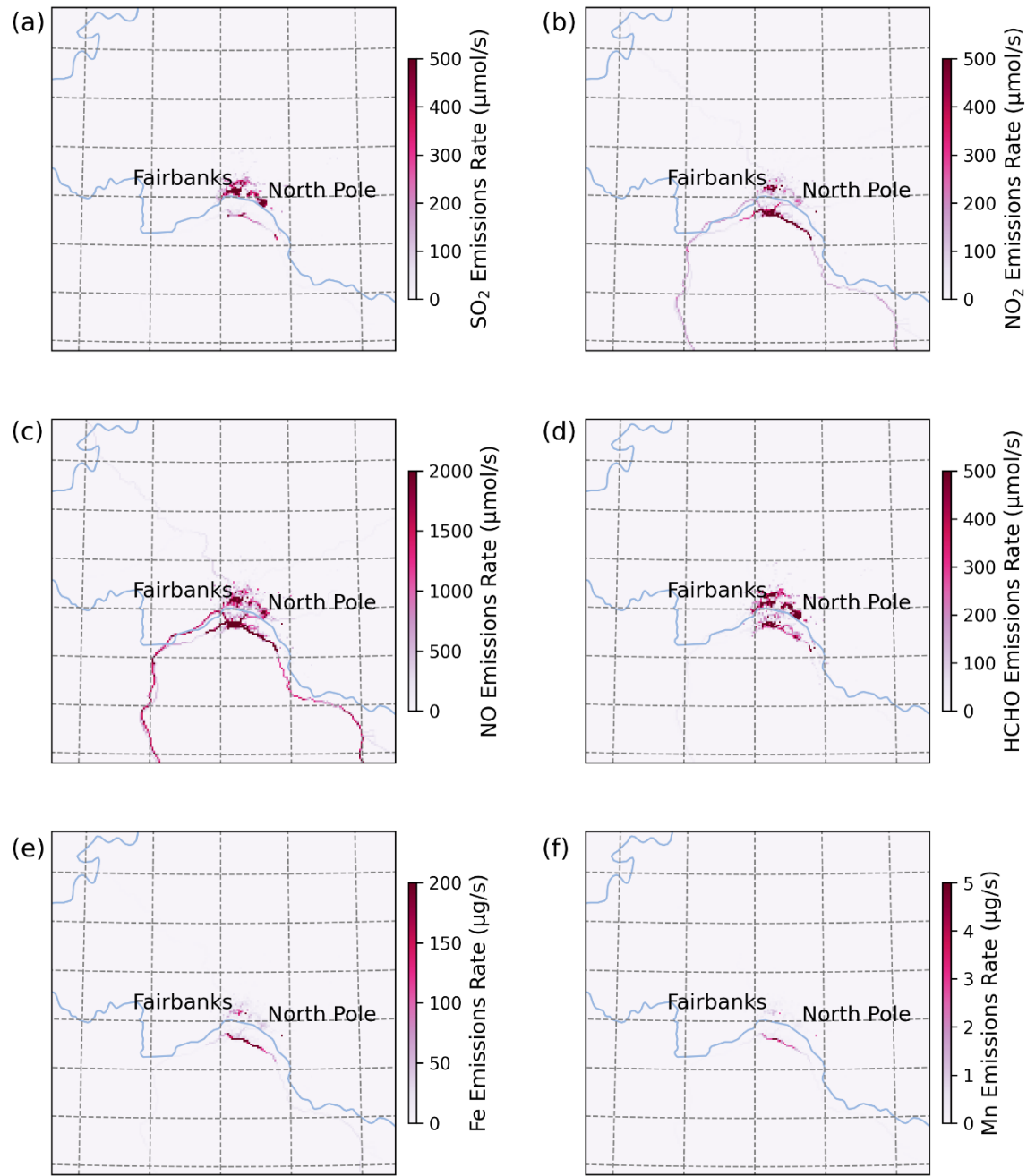
*Supplement of*

## **Predicted impacts of heterogeneous chemical pathways on particulate sulfur over Fairbanks (Alaska), the Northern Hemisphere, and the Contiguous United States**

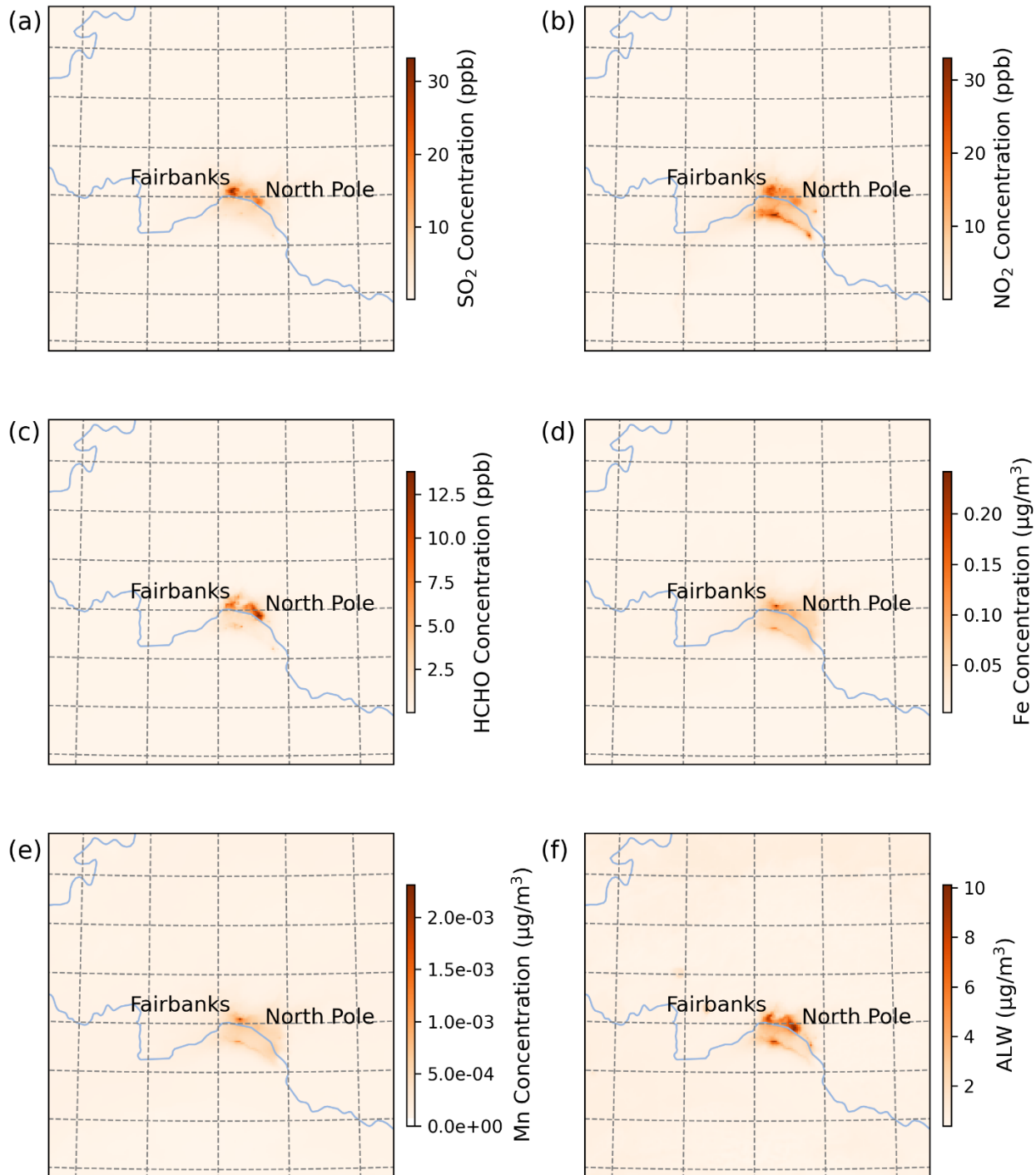
**Sara L. Farrell et al.**

*Correspondence to:* Sara L. Farrell (farrell.sara@epa.gov) and Kathleen Fahey (fahey.kathleen@epa.gov)

The copyright of individual parts of the supplement might differ from the article licence.



10 **Figure S1. Episode averaged emissions of particulate sulfur precursors for episode 1 (January 25th – February 11th, 2008) in the Fairbanks Domain.**



15 **Figure S2.** Episode averaged modelled ambient concentrations of PM2.5, sulfur precursors in the Base\_Het simulation for episode 1 (January 25<sup>th</sup> – February 11<sup>th</sup>, 2008) over the Fairbanks Domain.

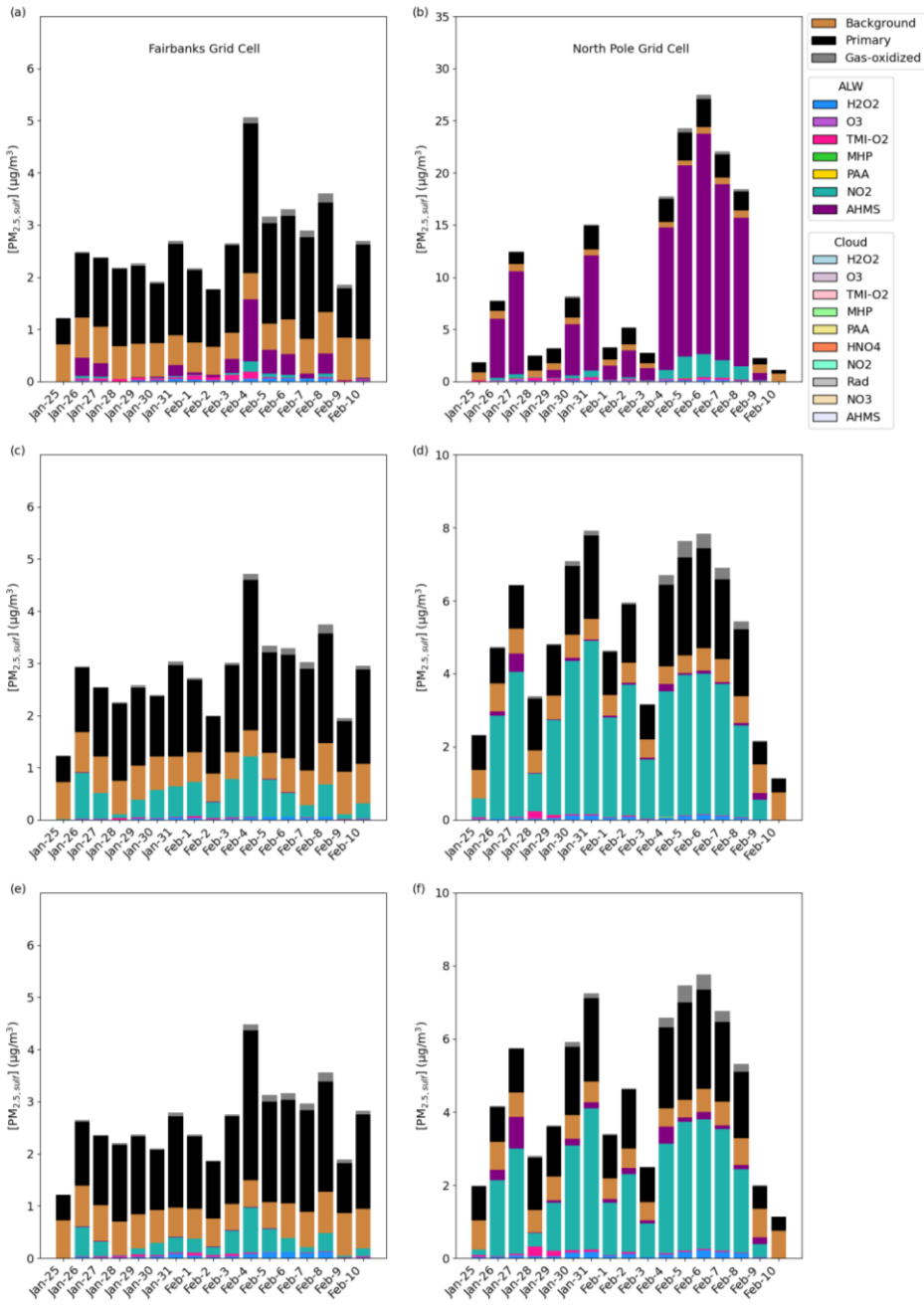
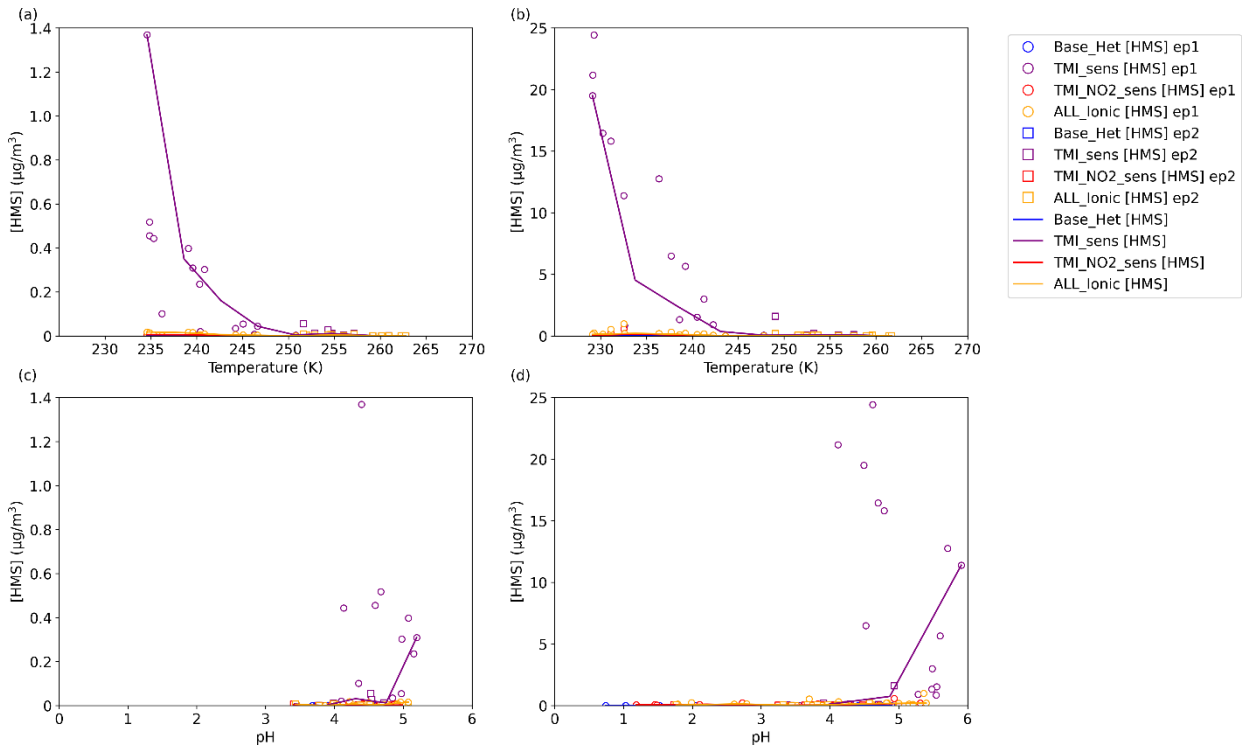


**Figure S3. Average daily  $[\text{PM}_{2.5,\text{sulf}}]$  concentrations in the TMI\_sens (a & b), TMI\_NO2\_sens (c & d), and All\_Ionic (e & f) simulations at Downtown Fairbanks (a, c & e) located at the State Office Building (64.84 N, -147.72 W; grid cell 108,93) and North Pole (b, d & f) located at (64.76 N, -147.34 W; grid cell 122, 86) for episode 1 speciated by source and/or formation pathway. Secondary aqueous formation of  $[\text{PM}_{2.5,\text{sulf}}]$  is broken out into two categories: ALW and Cloud, where ALW pathways represent the heterogeneous sulfur chemistry added in this study.**



25 **Figure S4.) Relationship between HMS formation and temperature (a & b) and HMS formation and pH (c & d) for the Fairbanks domain (both episodes) at the Downtown Fairbanks Grid Cell (a & c) and the North Pole Grid Cell (b & d). Scatters represent daily averages (17 points per model run for E1 and 12 points per model run for E2). Interpolated trend lines were calculated assuming a linear degree of B-spline at 8 intervals for HMS/Temperature relationships (a & b) and 5 intervals for HMS/pH relationships (c & d).**

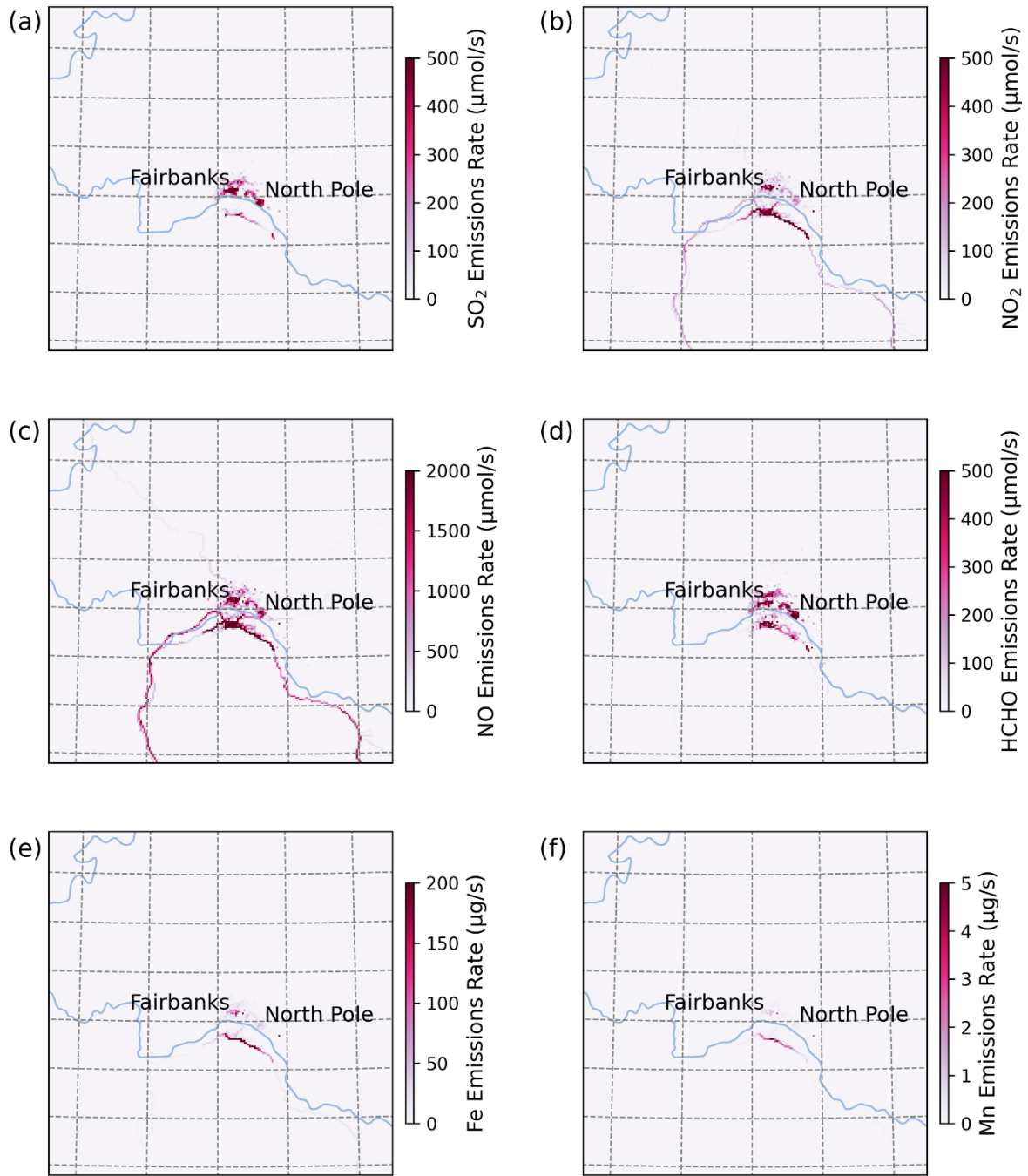


**Figure S5. Average emissions of sulfur aerosol precursors for episode 2 (November 4th – November 17th, 2008)**

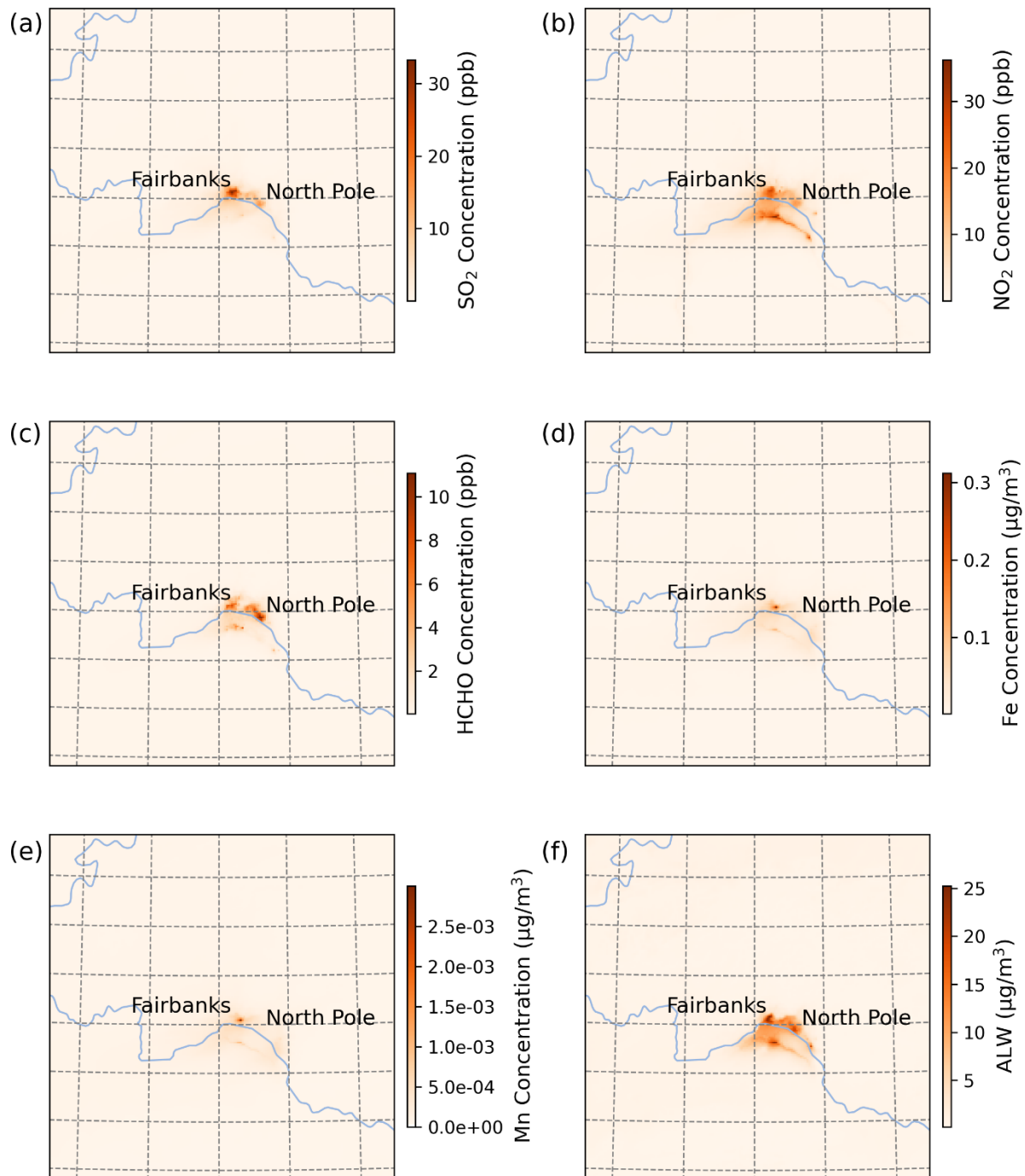


**Figure S6.** Episode averaged modelled ambient concentrations of PM2.5, sulfur precursors in the Base\_Het simulation for episode 2 (November 4th – 17th, 2008) over the Fairbanks Domain.

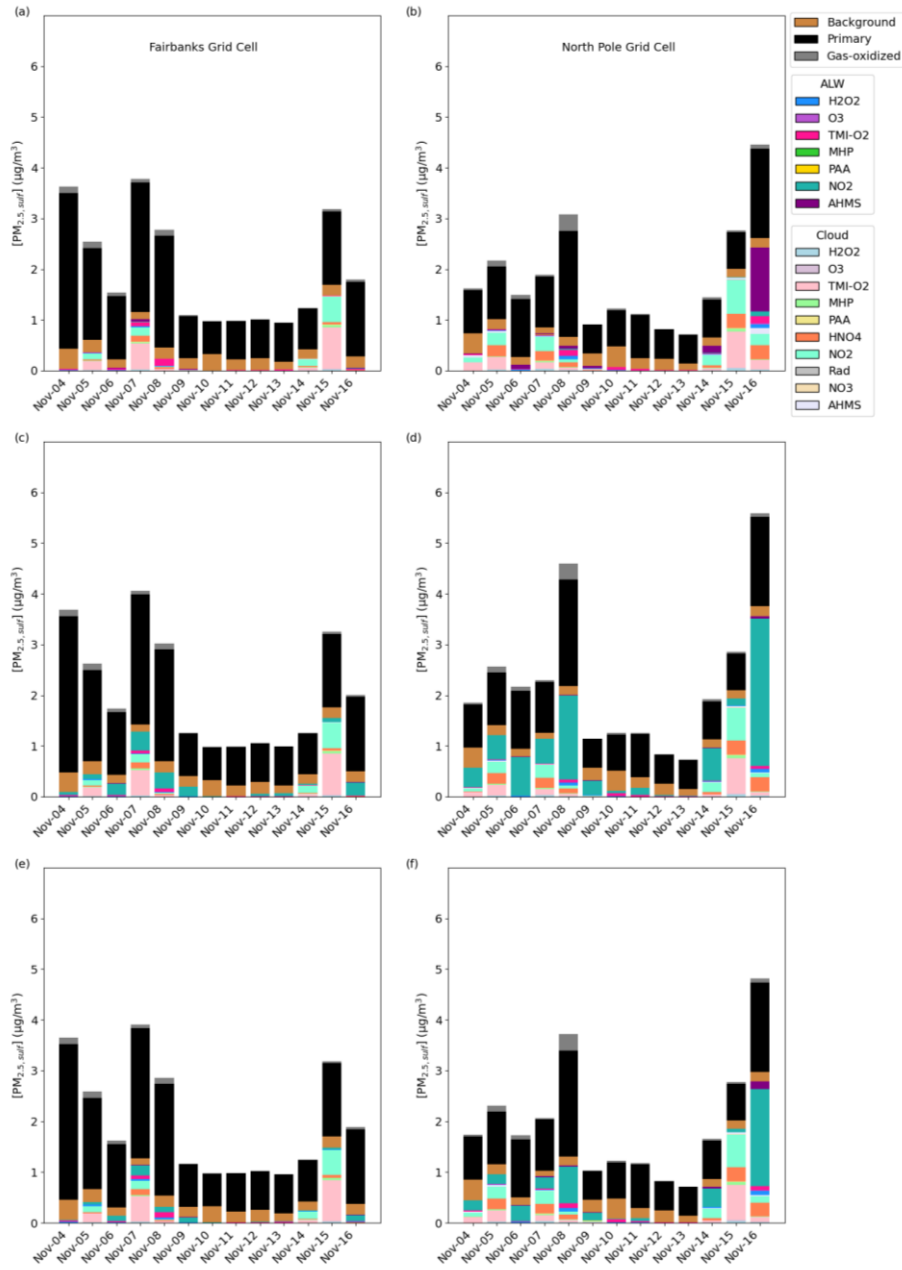
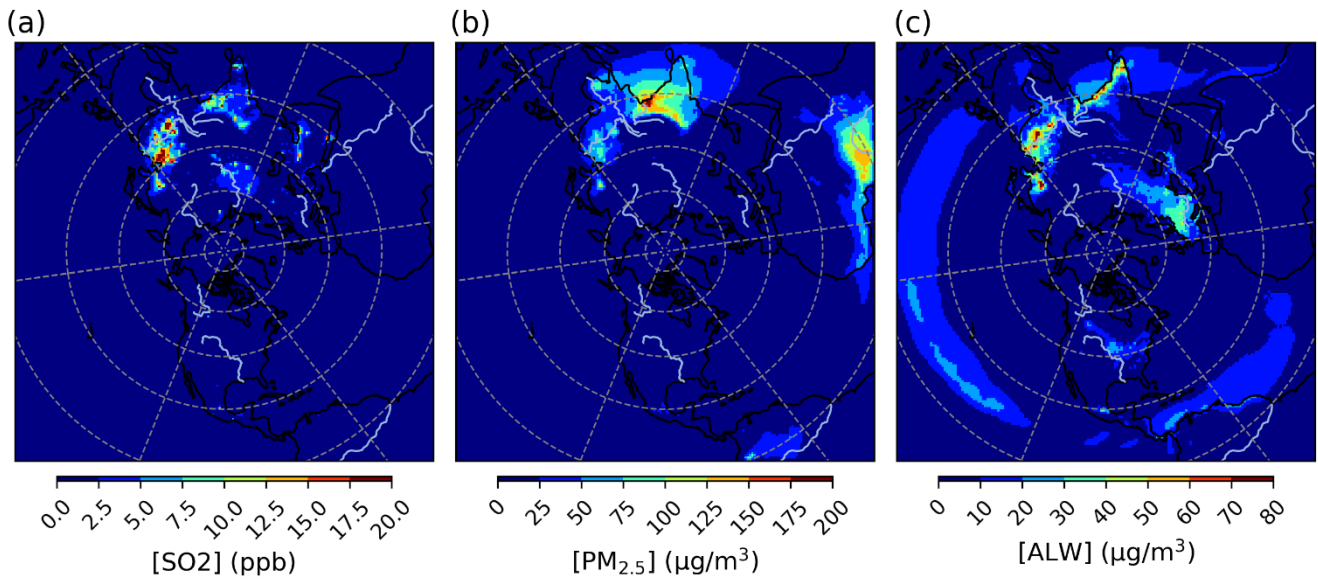


**Figure S7. Average daily PM<sub>2.5,sulf</sub> concentrations in the TMI\_sens (a & b), the TMI\_NO2\_sens (c & d), and the All\_Ionic (e & f) simulations at Downtown Fairbanks (a, c & e) located at the State Office Building (64.84 N, -147.72 W; grid cell 108,93) and North Pole (b, d & f) located at (64.76 N, -147.34 W; grid cell 122, 86) for episode 2 speciated by source and/or formation pathway. Secondary aqueous formation of PM<sub>2.5,sulf</sub> is broken out into two categories: ALW and Cloud, where ALW pathways represent the heterogeneous sulfur chemistry added in this study.**



50 **Figure S8. Episode Averaged SO<sub>2</sub> (a), PM<sub>2.5</sub> (b), and ALW (c) from Base HCMAQ for a wintertime episode (December 1st, 2015 – February 29th, 2016)**

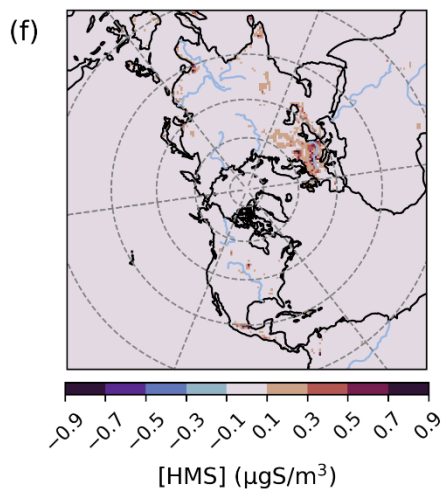
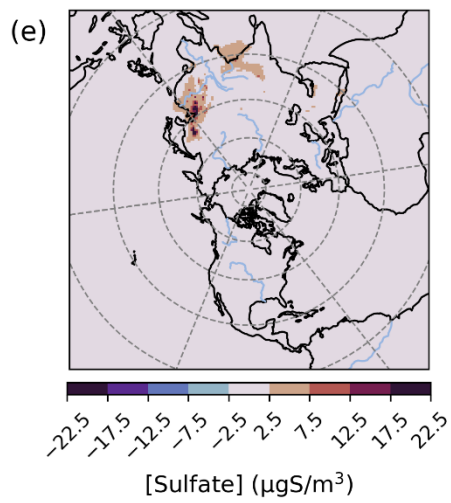
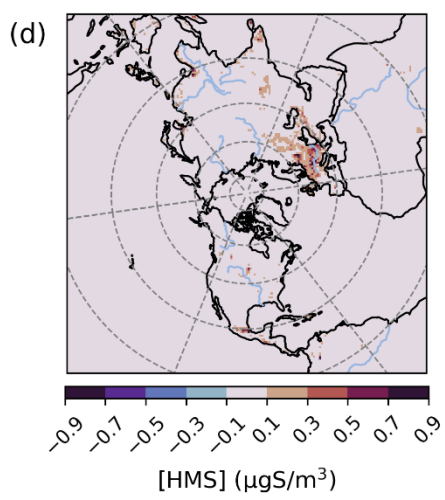
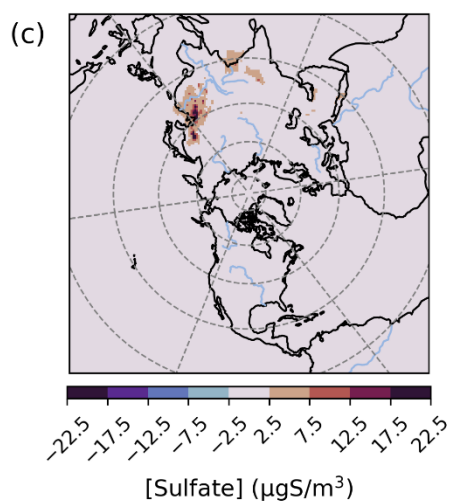
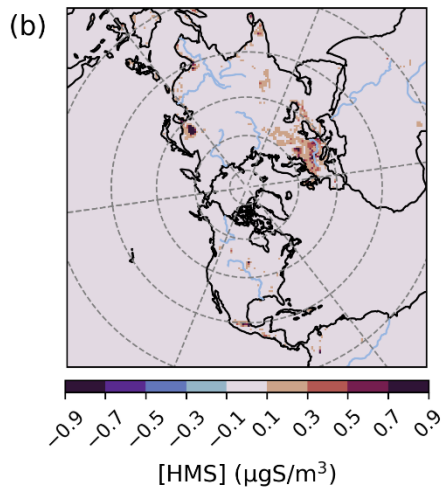
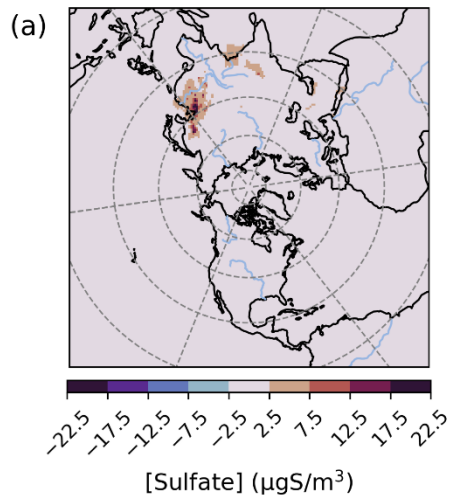


Figure S9. Maximum daily differences in sulfate and HMS for the TMI\_sens (a&b), the TMI\_NO2\_sens (c & d) and the All\_Ionic (e & f) model simulations over the HCMAQ N. Hemisphere domain for a wintertime episode (December 1st, 2015 – February 29th, 2016). Differences are cast in micrograms of sulfur per meter cubed to be consistent with measurement units from EMEP.

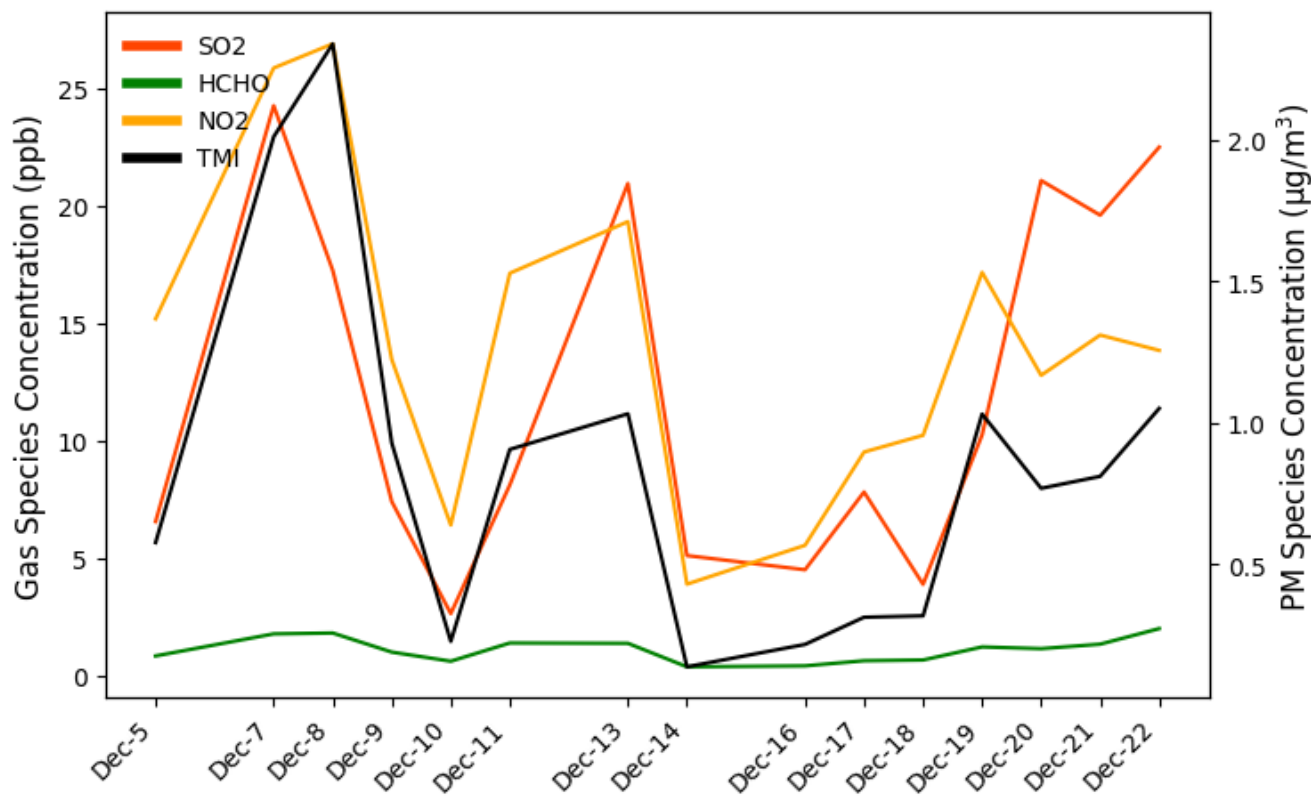
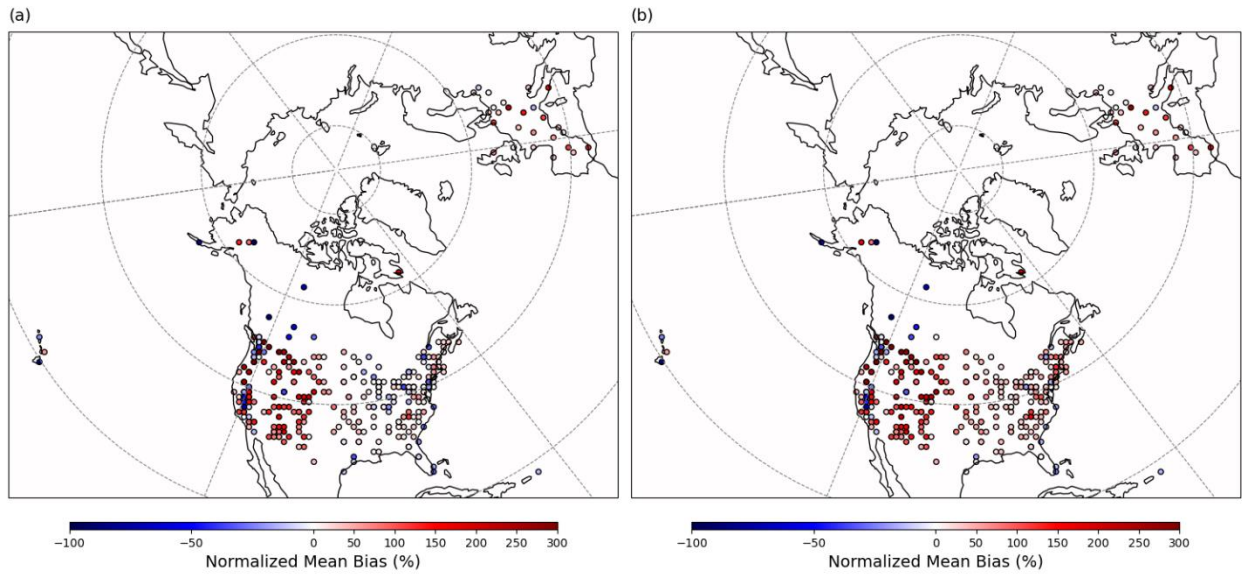
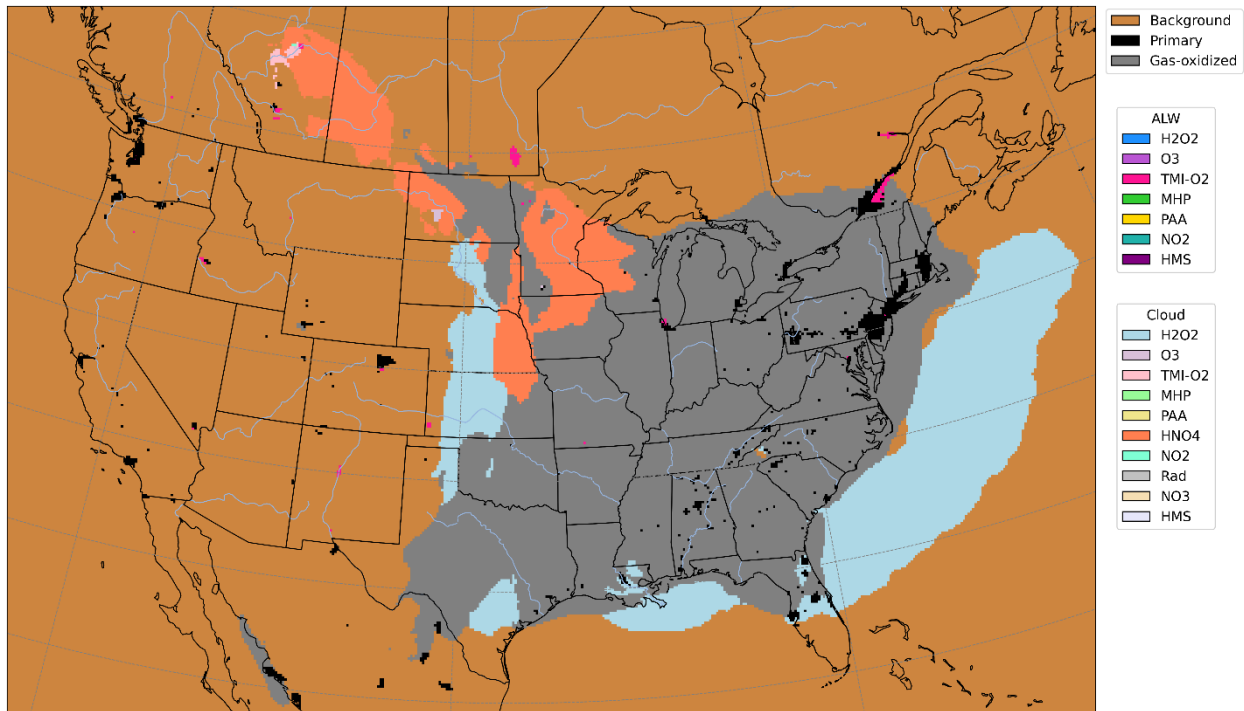


Figure S10. Time series of daily averaged secondary sulfate formation oxidant and catalyst concentrations for Base HCMAQ at a grid cell over Tsinghua University in Beijing, China from December 5<sup>th</sup> to December 22<sup>nd</sup>, 2015.



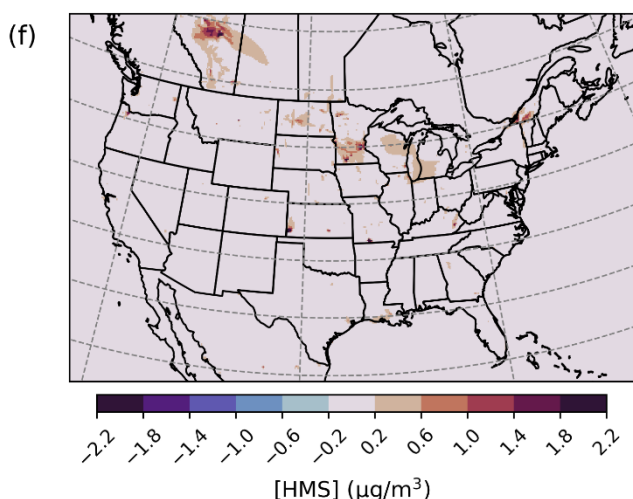
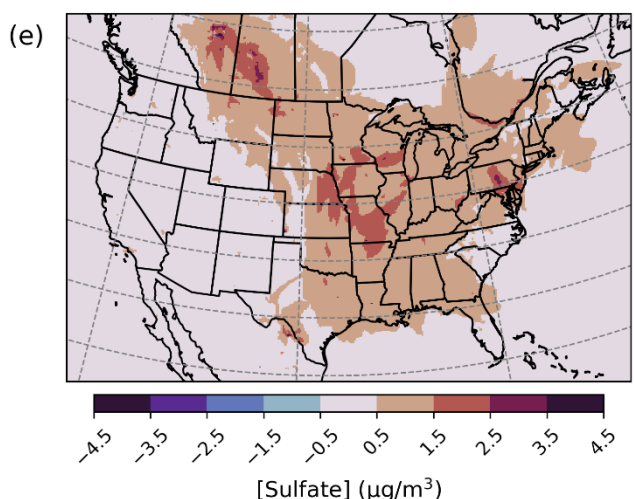
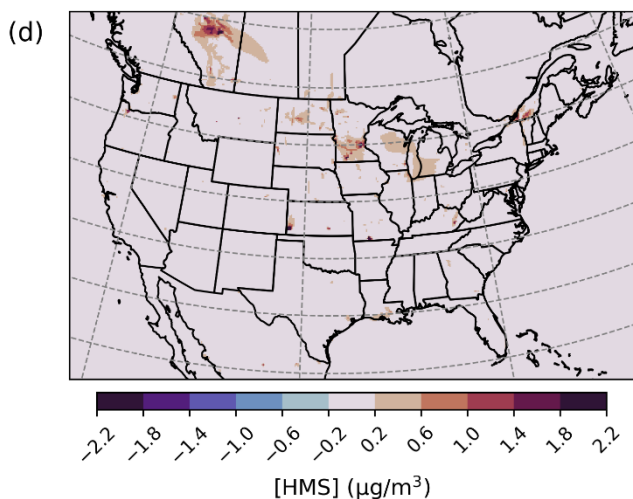
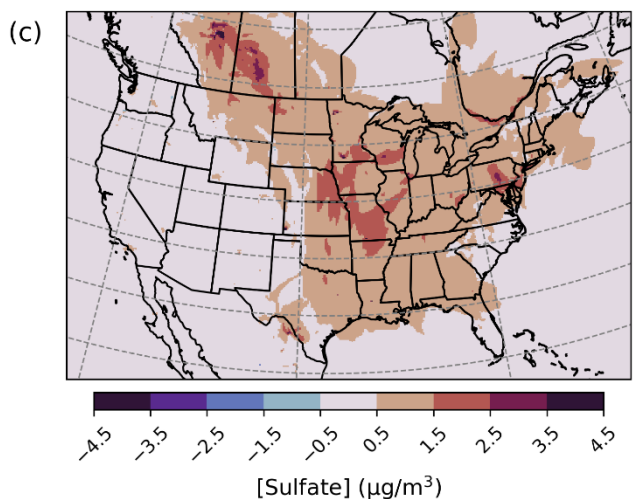
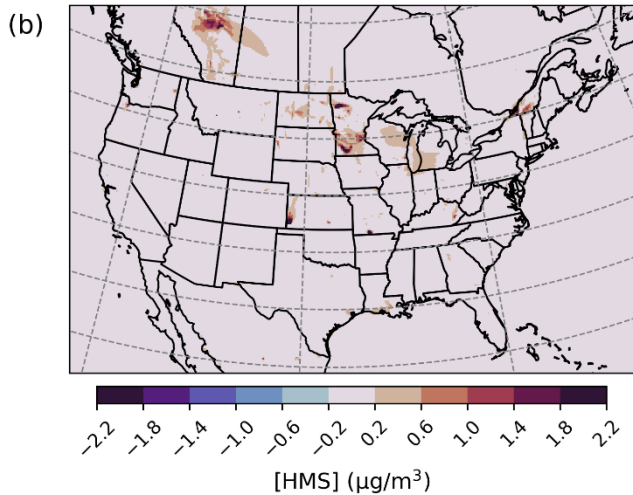
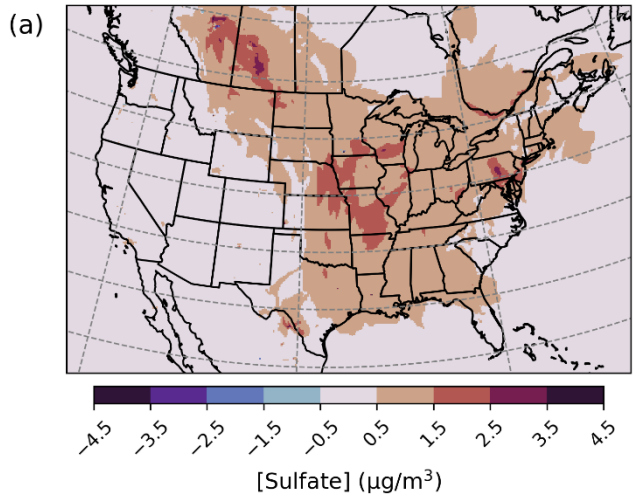
65

**Figure S11.** Normalized Mean Bias for  $\text{PM}_{2.5,\text{sulf}}$  by monitor over the Hemispheric Domain for the winter season 2015-2016 for the Base (a) and Base\_Het (b) model simulations.



70 **Figure S12.** Leading contributor to  $\text{PM}_{2.5,\text{sulf}}$  concentration for January 2016 over CONUS in the Base\_Het model simulation.





75 **Figure S13. Maximum daily differences in sulfate and HMS between Base CMAQ and the TMI\_sens (a&b), the TMI\_NO2\_sens (c & d), and the All\_Ionic (e & f) simulations for a wintertime episode (January 2016). HMS formation was not included in Base CMAQ, and HMS mass concentrations are multiplied by the ratio of sulfate to HMS molecular mass.**

80

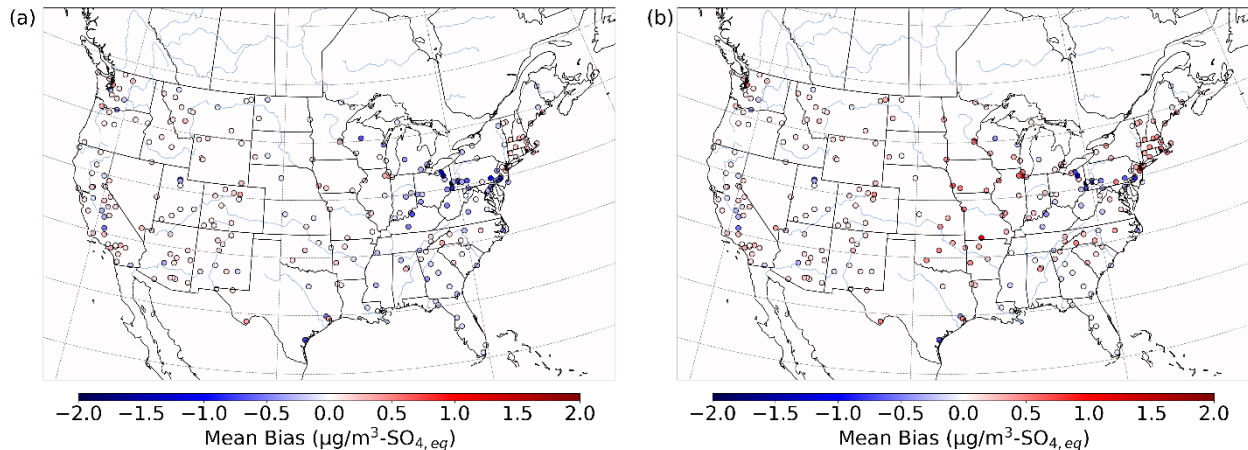
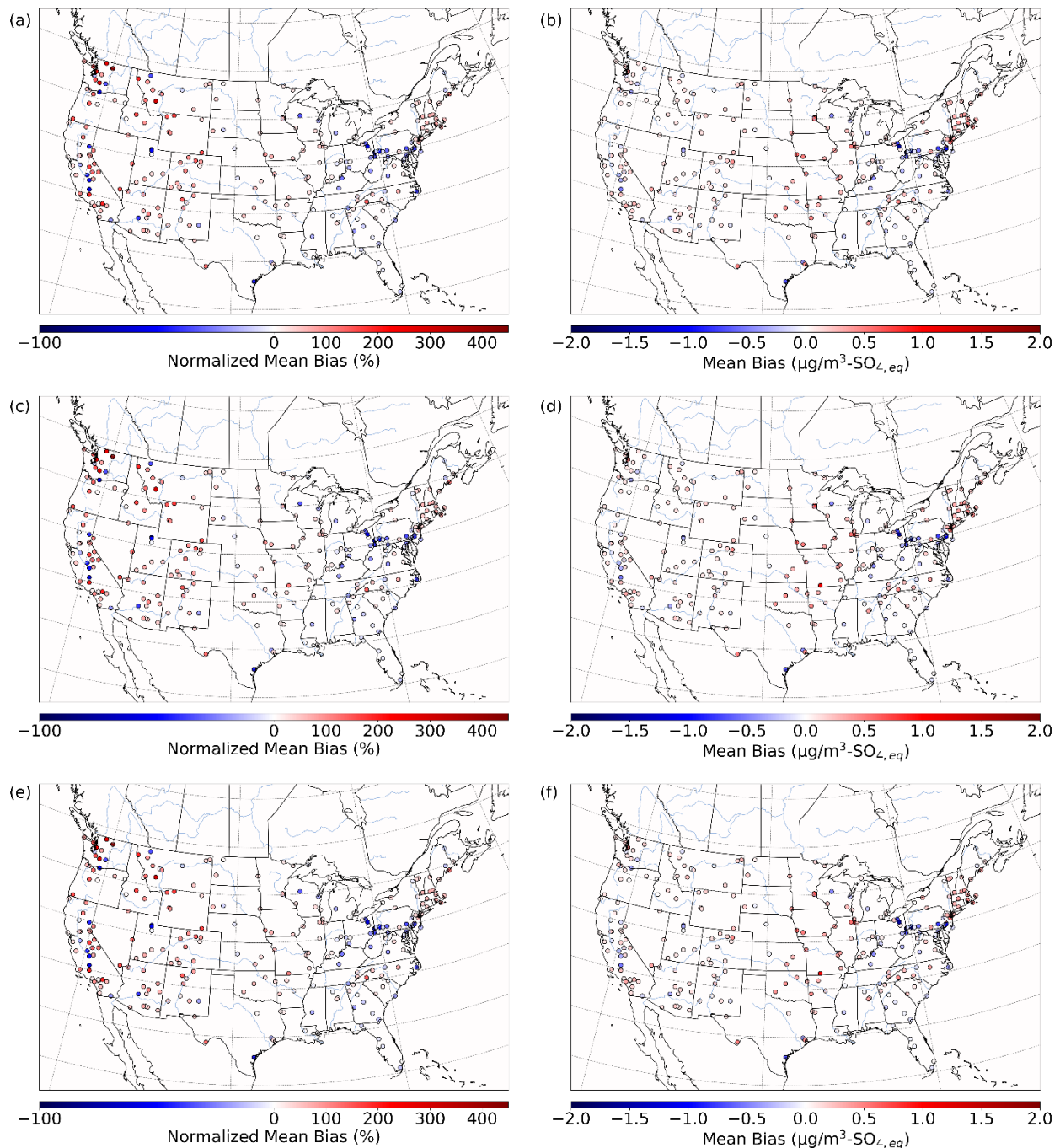
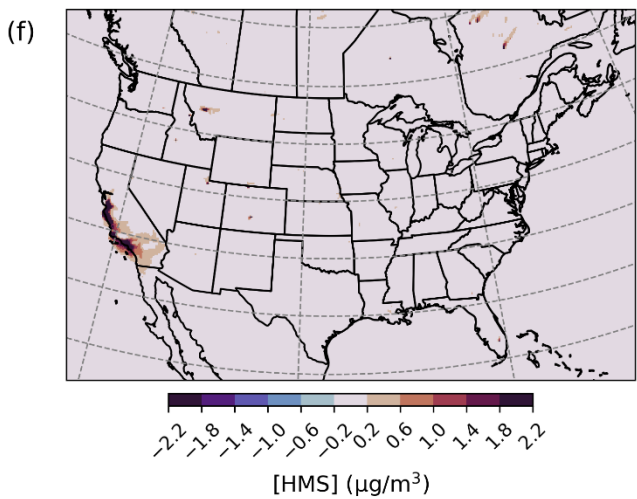
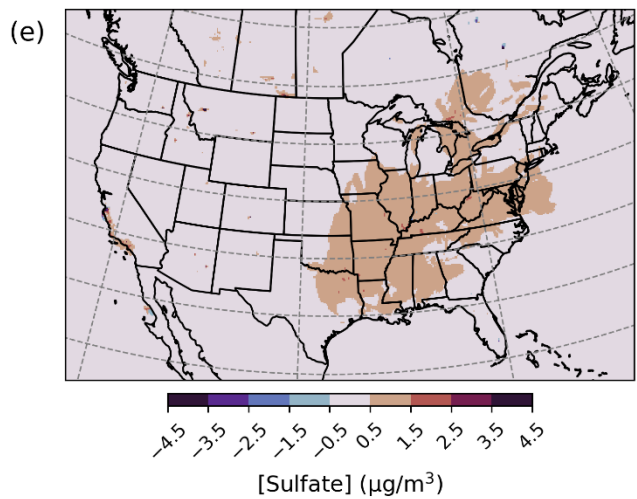
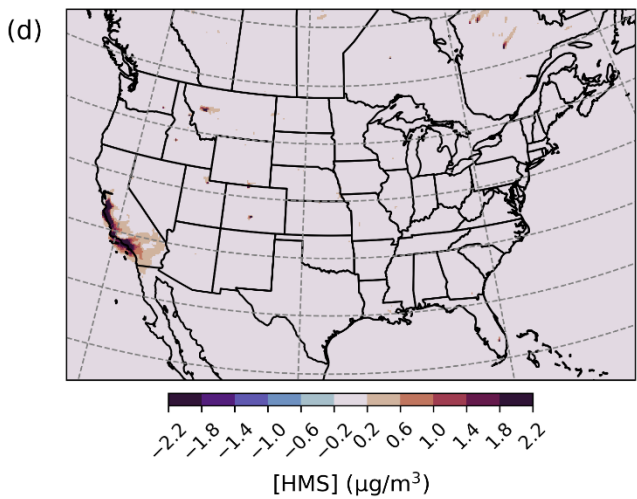
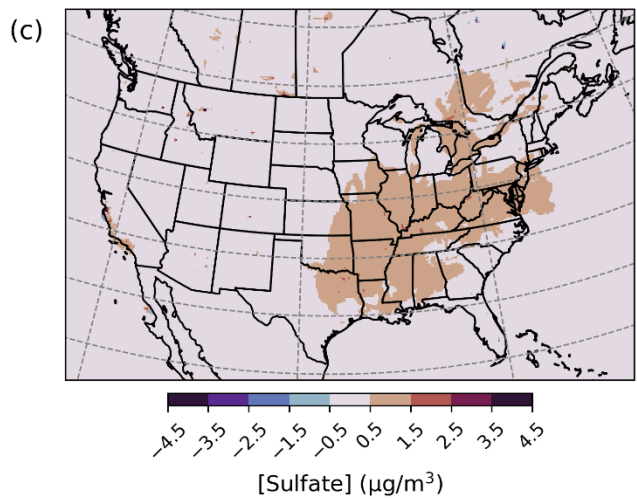
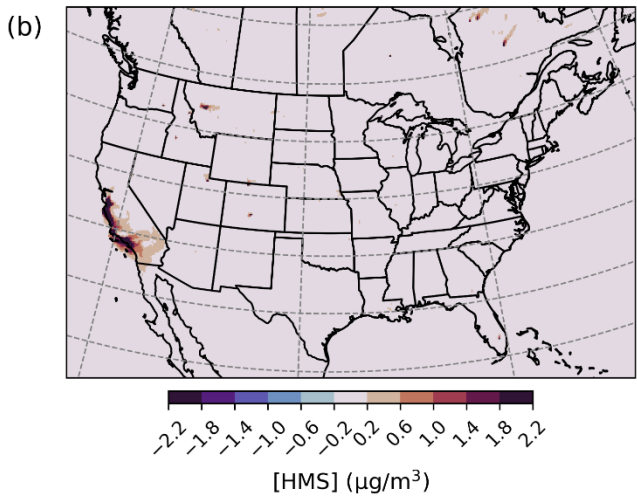
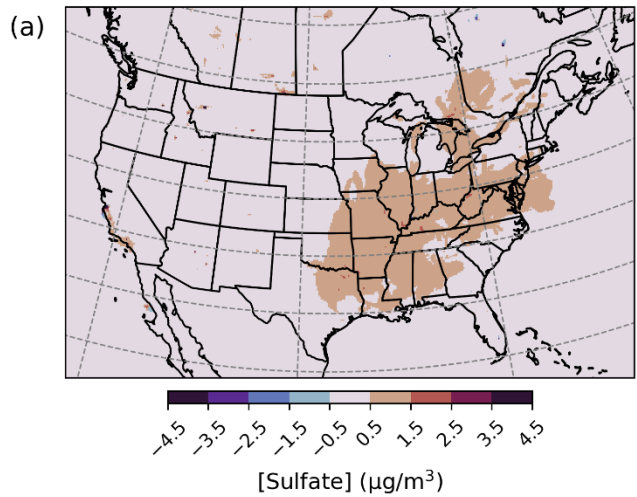


**Figure S14. Mean bias calculated for modelled PM2.5,sulf in the Base (a) and Base\_Het (b) simulation for a wintertime episode (January 2016) over the CONUS domain. Mean bias is cast in  $\text{SO}_4$  equivalence to account for and equate HMS contributions to sulfate measured mass in observations (HMS modelled concentrations are multiplied by the ratio of sulfate to HMS molecular mass).**

85



90 **Figure S15. Normalized mean bias and mean bias in modelled PM<sub>2.5,sulf</sub> for a wintertime episode (January 2016) over the CONUS domain predicted by the TMI\_sens (a & b), the TMI\_NO2\_sens (c & d), and the All\_Ionic (e & f) simulations. Mean bias is cast in SO<sub>4</sub> equivalence to account for and equate HMS contributions to sulfate measured mass in observations.**



95 **Figure S16. Max daily differences in sulfate and HMS between Base CMAQ and the TMI\_sens (a & b), the TMI\_NO2\_sens (c & d),  
and the All\_Ionic (e & f) simulations for a summertime episode (July 2016).**

100

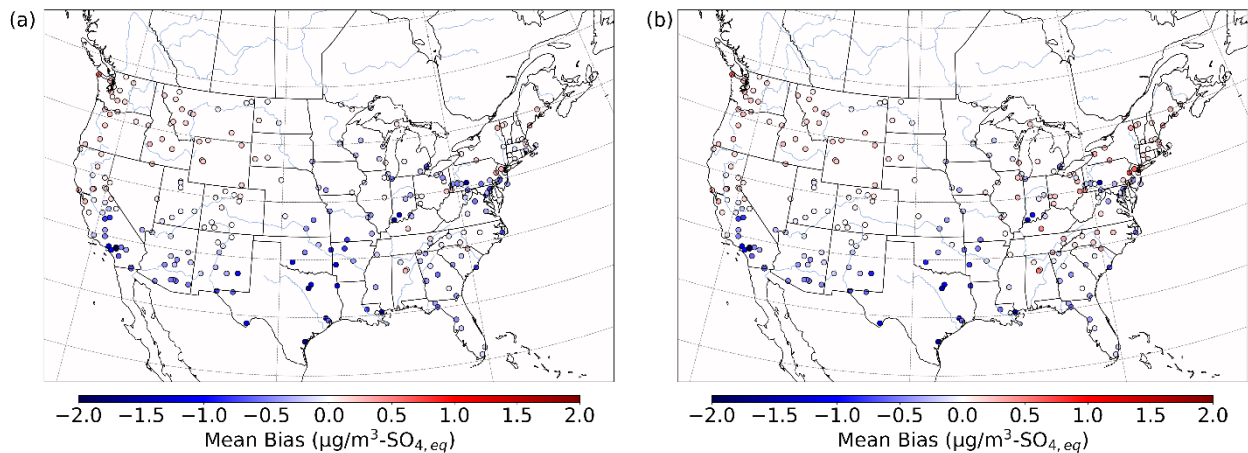


**Figure S17. Mean bias calculated for modelled PM<sub>2.5,sulf</sub> in the Base (a) and Base\_Het (b) simulation for a summertime episode (July 2016) over the CONUS domain. Mean bias is cast in SO<sub>4</sub> equivalence to account for and equate HMS contributions to sulfate measured mass in observations.**

105

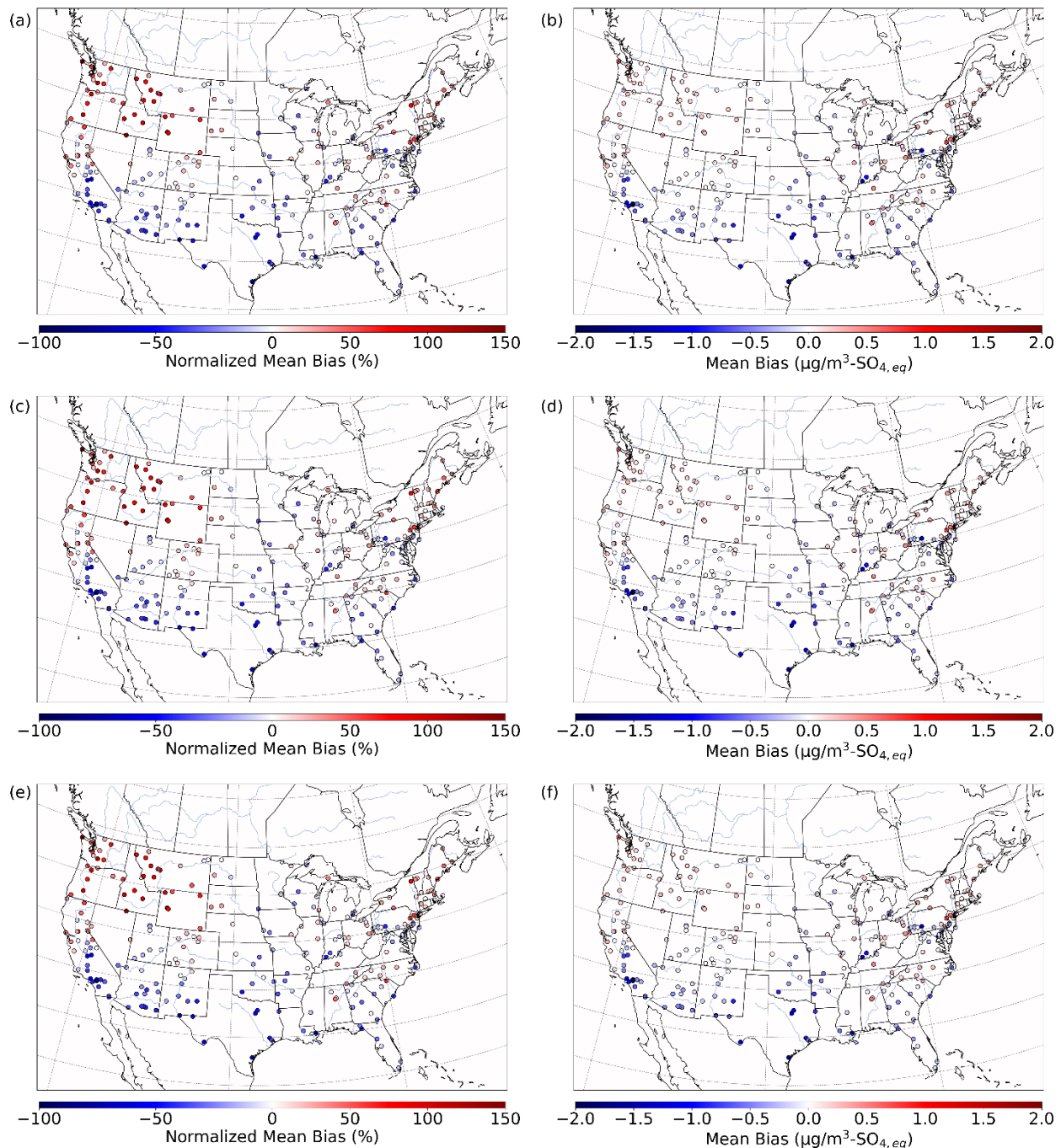


**Figure S18. Normalized mean bias and mean bias in modelled PM<sub>2.5,sulf</sub> for a summertime episode (July 2016) over the CONUS domain predicted by the TMI\_sens (a & b), the TMI\_NO2\_sens (c & d), and the All\_Ionic (e & f) simulations.**

**Table S1. HCMAQ model performance metrics for all model runs by region, including, normalized mean bias (NMB), normalized mean error (NME), mean bias (MB), mean error (ME), root mean square error (RMSE), correlation coefficient (R2) and total observation-model match counts (n).**

Region	Performance	Base	Base_Het	TMI_sens	TMI_NO2_sens	All_IONIC
Canada	NMB (%)	-14.23	7.38	4.31	4.51	4.60
	NME (%)	50.00	56.54	54.97	55.01	55.00
	MB ( $\mu\text{g}/\text{m}^3$ )	-0.04	0.02	0.01	0.01	0.01
	ME ( $\mu\text{g}/\text{m}^3$ )	0.15	0.17	0.17	0.17	0.17
	RMSE ( $\mu\text{g}/\text{m}^3$ )	0.29	0.31	0.30	0.30	0.30
	R <sup>2</sup>	0.17	0.19	0.20	0.20	0.20
	n	421				
Europe	NMB (%)	25.35	26.93	26.75	26.80	26.15
	NME (%)	64.40	64.38	64.41	64.42	63.98
	MB ( $\mu\text{g}/\text{m}^3$ )	0.07	0.08	0.08	0.08	0.07
	ME ( $\mu\text{g}/\text{m}^3$ )	0.18	0.18	0.18	0.18	0.18
	RMSE ( $\mu\text{g}/\text{m}^3$ )	0.32	0.32	0.32	0.32	0.31
	R <sup>2</sup>	0.21	0.24	0.23	0.23	0.24
	n	3402				
USA	NMB (%)	12.70	36.08	33.85	33.89	33.95
	NME (%)	61.19	73.04	71.97	71.97	71.90
	MB ( $\mu\text{g}/\text{m}^3$ )	0.03	0.08	0.08	0.08	0.08
	ME ( $\mu\text{g}/\text{m}^3$ )	0.14	0.17	0.16	0.16	0.16
	RMSE ( $\mu\text{g}/\text{m}^3$ )	0.24	0.27	0.27	0.27	0.27
	R <sup>2</sup>	0.28	0.30	0.30	0.30	0.30
	n	7422				